

# Physics-Informed Multi-Agent Reinforcement Learning for Distributed Multi-Robot Problems

Eduardo Sebastián, Thai Duong, Nikolay Atanasov, Eduardo Montijano and Carlos Sagüés

**Abstract**—The networked nature of multi-robot systems presents challenges in the context of multi-agent reinforcement learning. Centralized control policies do not scale with increasing numbers of robots, whereas independent control policies do not exploit the information provided by other robots, exhibiting poor performance in cooperative-competitive tasks. In this work we propose a physics-informed reinforcement learning approach able to learn distributed multi-robot control policies that are both scalable and make use of all the available information to each robot. Our approach has three key characteristics. First, it imposes a port-Hamiltonian structure on the policy representation, respecting energy conservation properties of physical robot systems and the networked nature of robot team interactions. Second, it uses self-attention to ensure a sparse policy representation able to handle time-varying information at each robot from the interaction graph. Third, we present a soft actor-critic reinforcement learning algorithm parameterized by our self-attention port-Hamiltonian control policy, which accounts for the correlation among robots during training while overcoming the need of value function factorization. Extensive simulations in different multi-robot scenarios demonstrate the success of the proposed approach, surpassing previous multi-robot reinforcement learning solutions in scalability, while achieving similar or superior performance (with averaged cumulative reward up to  $\times 2$  greater than the state-of-the-art with robot teams  $\times 6$  larger than the number of robots at training time).

**Index Terms**—Cooperative control, distributed systems, multi-robot systems, physics-informed neural networks, reinforcement learning.

## I. INTRODUCTION

**M**ULTI-ROBOT systems promise improved efficiency and reliability compared to single robots in many applications, including exploration and mapping [1], [2], agriculture and herding [3]–[6], and search and rescue [7]. However, the complexity of describing mathematically the objective and constraints in many of these problems makes the design of analytical controllers a challenging task. Multi-agent reinforcement learning [8]–[12] addresses this issue by only requiring a high-level mathematical specification of the task (the reward function), which is commonly available.

E. Sebastián, E. Montijano and C. Sagüés are with the DIIS - I3A, Universidad de Zaragoza, Spain (e-mails: {esebastian, emonti, csagues}@unizar.es).

T. Duong and N. Atanasov are with the Department of Electrical and Computer Engineering, University of California San Diego, La Jolla, CA 92093 USA (e-mails: {tduong, natanasov}@ucsd.edu).

This work has been supported by ONR N00014-23-1-2353 and NSF CCF-2112665 (TILOS), by Spanish projects PID2021-125514NB-I00, PID2021-124137OB-I00 and TED2021-130224B-I00 funded by MCIN/AEI/10.13039/501100011033, by ERDF A way of making Europe and by the European Union NextGenerationEU/PRTR, DGA T45-23R, and Spanish grant FPU19-05700.

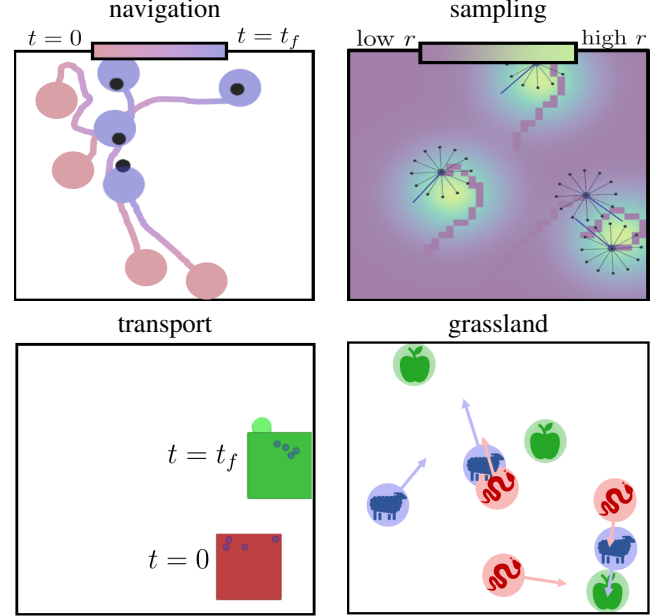


Fig. 1. Examples of scenarios addressed by our physics-informed multi-agent reinforcement learning approach. The scenarios cover a wide variety of cooperative/competitive behaviors and levels of coordination complexity.

A fundamental limitation of existing multi-agent reinforcement learning approaches is the poor scalability they offer against increasing and time-varying numbers of robots. Centralized control policies do not scale whereas independent control policies neglect the information that other robots can offer. How to design and train control policies based on neural networks that are distributed and use all the available information is still an open problem [11], [13], [14]. The approach explored in this paper leverages physical knowledge about the robot system [15]–[20] to make this possible. Physics-informed neural networks are becoming popular in different fields, e.g., climate science, quantum mechanics or fluid dynamics [21], [22]. They need less data for training and allow encoding general constraints found in physical systems. Nonetheless, they have not been used to learn distributed multi-robot control policies in multi-agent reinforcement learning.

The main contribution of our work is a novel physics-informed multi-agent reinforcement learning approach suitable for general multi-robot problems (Sec. III). The techniques to make this possible (Sec. IV) are summarized as follows.

- We develop a novel distributed and scalable by design neural network architecture to describe multi-robot control policies. This is achieved by combining a physics-informed port-Hamiltonian description of the multi-robot system (Sec. IV-A) with self-attention (Sec. IV-B). The

former naturally encodes the distributed nature of the policy and respects the energy conservation laws of the individual dynamics of the robots. The latter handles the information coming from communication or perception in time-varying neighborhoods.

- We integrate the port-Hamiltonian self-attention policy in a soft actor-critic reinforcement learning algorithm that exploits the physics-informed description of the robot team to impose the sparsity pattern from the interaction graph in the policy function (Sec. V). To handle the networked nature of the multi-robot policy and avoid non-stationarity issues during training, we modify the acquisition of experience to keep track of the correlations among robots.

Extensive simulations in different multi-robot scenarios (Sec. VI) demonstrate that the combination of multi-agent reinforcement learning techniques and a physics-informed description of the system achieves scalable control policies with similar or superior performance as the state-of-the-art (Sec. VII).

This paper is an extension of a conference paper in [17]. This paper addresses multi-robot problems where only a reward specification of the task is given, whereas [17] considers that data from an expert controller is available. In that sense, [17] is more closely related to inverse reinforcement learning, while this paper considers a reinforcement learning setting. The proposed approach is also different. Specifically, we propose a novel multi-agent reinforcement learning approach where the control policy is conditioned on the interaction graph of the multi-robot system by exploiting a port-Hamiltonian formulation and a self-attention-based parameterization, while [17] reduces to a supervised learning approach. The neural networks that model the control policies are different as well, since the multi-agent reinforcement learning scenarios are continuous-time while the datasets in [17] are discrete-time. Finally, all experiments in this paper are new.

## II. RELATED WORK

### A. Learning multi-robot control policies from data

The design of multi-robot control policies deals with two challenges.

The first challenge is the mathematical formulation of the problem, where we must consider the task and the constraints inherited from the cooperative-competitive nature of the multi-robot team. To address this, recent works exploit machine learning and focus on learning control policies for optimal control or reinforcement learning problems [23]–[25]. When demonstrated data from an expert are available, inverse reinforcement learning [26] can be used to learn centralized [27], [28] or distributed [29], [30] policies from task demonstrations. However, finding experts for multi-robot applications is difficult. It is also possible to apply supervised learning approaches to learn multi-robot control policies [31], [32], but, again, collecting labeled trajectories is hard. Therefore, in this work we use reinforcement learning, because a reward

function is a high-level description of the task that is easy to build and is typically available.

The second challenge is that the learning and execution of control policies for multi-robot systems should scale favorably with an increasing numbers of robots. Learning a joint policy function is challenging due to the exponential growth of the state and action space [33]. Attention mechanisms are widely used in multi-agent reinforcement learning problems [34]–[37] to enhance the performance of centralized training settings where the agents are isolated from each other and do not consider communication during deployment. Graph neural networks [11] have been utilized as a stable [38], scalable and communication-aware policy representation in path planning, coverage, exploration, and flocking problems [39]–[44]. These approaches assume discrete robot dynamics, fixed or known communication topology, or prior knowledge on the formulation of the control policy. In contrast, by using a port-Hamiltonian formulation and self-attention mechanisms, our approach directly learns control policies that handle time-varying neighbors, do not constrain the size of the neighborhoods, and learn constraints such as collision avoidance without specific mathematical formulation.

### B. Multi-agent reinforcement learning for robotic problems

Multi-agent reinforcement learning extends reinforcement learning approaches to problems where multiple agents interact in the environment [45]–[50]. The first multi-agent reinforcement learning approaches considered centralized policies where the states, actions and observations of every agent are globally known by a central unit during deployment [8]. The complexity of these approaches exponentially scales with the number of agents, so they are not feasible in practice. In the absence of a centralized policy, the Markov game modeling the problem becomes non-stationary [51]–[53]. The task is no longer stationary because the policies of all the other agents are changing, and so the environment itself. As a consequence, it is not possible to reach an equilibrium in training.

To solve the non-stationarity issue, the common approach is to factorize the value and/or policy functions. The most extended factorization, the so-called centralized-training decentralized-execution, departs from centralized-training reinforcement learning approaches [54]–[56] and considers that the agents act independently. To do so, the agents can learn an approximation of the other agents' control policies [57]. The resulting control policies only use the individual observations; by neglecting communications, the performance barely scales with the number of robots. Another option is to provide each agent with a global estimator that predicts the trajectories of the whole multi-robot team [58] or to implicitly learn to coordinate with other agents through the value function [53]. In mean field approaches [59], the multi-agent game is reduced to an interaction between an agent and the average of the other agents, which is not practical. To overcome these issues, we propose a new formulation of the policy function that is distributed by design and captures the underlying interaction graph that describes the multi-robot system.

Other works focus on more complex factorizations that account for the local interactions among neighboring agents

in the value function. For instance, the value function can be approximated as dependent on the neighbors only [60]. Either from analytical [14], [33] or learned [61]–[63] factorizations, the learned control policies are still restricted to the same team size used during training because the policies do not explicitly consider communication. By using a port-Hamiltonian description of the system, our approach avoids to approximate the reward, value or policy functions by any factorization, thus fully exploiting the available information in the experience while learning scalable distributed control policies.

### C. Physics-informed neural networks for robotic problems

While black-box neural networks are widely used for learning control policies, they do not encode energy conservation and kinematic constraints satisfied by physical robot systems. Failing to infer them from data may result in unstable behaviors. Moreover, other constraints are present that come from the perception and communication modules of the robots and which restrict the information available to the robot. Similar issues are found in other physical applications [22], leading to physics-informed neural network [21], neural networks that use the differential equations that model physical systems as building blocks. The use of physics-informed machine learning for robotics and control is very recent [18]–[20], [64], [65] and focuses on centralized controllers. Nevertheless, physics-informed neural network can also be used to address the learning of cooperative distributed control policies.

Many dynamical systems—from robots interacting with their surroundings to large-scale multi-physics systems—involve a number of interacting subsystems. This compositional property can be exploited [16] to train neural network sub-models from data generated by simple sub-systems, and the dynamics of more complex composite systems are then predicted without requiring additional data. The systems are represented as a port-Hamiltonian neural network [15], a class of neural ordinary differential equations that uses a port-Hamiltonian dynamics formulation as inductive bias [66]. A key contribution of our work is to represent the robot team as a port-Hamiltonian system and learn distributed control policies by modeling robot interactions as energy exchanges. The use of Hamiltonian mechanics has been explored for centralized control policies or distributed but fixed-time known topologies [67]–[69]. Meanwhile, our work achieves scalability with a time-varying topology by modeling robot interactions using self-attention [70].

## III. PROBLEM FORMULATION

Consider a team of robots, indexed by  $\mathcal{V} = \{1, \dots, n\}$ . The robot team motion is governed by *known* continuous-time control-affine stochastic dynamics:

$$\dot{\mathbf{x}}(t) = \mathbf{f}(\mathbf{x}(t), \mathbf{u}(t)) + \mathbf{L}\omega(t), \quad (1)$$

where  $\mathbf{x}(t) = [(\mathbf{x}^1(t))^\top, \dots, (\mathbf{x}^n(t))^\top]^\top \in \mathcal{X} \subseteq \mathbb{R}^{n \times n_x}$  is the joint state of the robot team at time  $t \geq 0$ , with  $\mathbf{x}^i(t)$  the state of robot  $i$  at time  $t$ . On the other hand,  $\mathbf{u} = [(\mathbf{u}^1(t))^\top, \dots, (\mathbf{u}^n(t))^\top]^\top \in \mathcal{U} \subseteq \mathbb{R}^{n \times n_u}$  is the joint input, with  $\mathbf{u}^i(t)$  the input of robot  $i$  at time  $t$ . The term  $\omega(t)$

is white noise modeling the uncertainty in the robot sensors and actuators and  $\Xi = \mathbf{L}\mathbf{L}^\top$  is the noise diffusion matrix. Let  $\{t_\tau\}_{\tau=0}^\infty$  be a sequence of discrete time instants such that  $t_{\tau+1} - t_\tau = T > 0$  and assume zero-order hold inputs such that  $\mathbf{u}(t) = \mathbf{u}(t_\tau)$ ,  $\forall t \in [t_\tau, t_{\tau+1})$ . Then, from Eq. (1), we can obtain an Euler discretization of the dynamics with discrete-time state  $\mathbf{s}_\tau = \mathbf{x}(t_\tau)$ , action  $\mathbf{a}_\tau = \mathbf{u}(t_\tau)$ , and dynamics:

$$\mathbf{s}_{\tau+1} = \mathbf{s}_\tau + T\mathbf{f}(\mathbf{s}_\tau, \mathbf{a}_\tau) + \mathbf{n}_\tau, \quad (2)$$

where  $\mathbf{n}_\tau$  is zero-mean Gaussian noise with covariance  $T\Xi$ . We will formulate the dynamics  $\mathbf{f}$  using port-Hamiltonian mechanics as its modularity in terms of energy effectively describes the networked interactions in a robot team.

The multi-robot task and the interactions among the robots are modeled as a Markov Decision Process (MDP), defined as a tuple  $(\mathcal{X}, \mathcal{U}, p, r, \gamma)$ . In the tuple,  $p : \mathcal{X} \times \mathcal{X} \times \mathcal{U} \rightarrow \mathbb{R}$  is the probability density of the next joint state  $\mathbf{s}_{\tau+1}$  conditioned on the current joint state  $\mathbf{s}_\tau$  and joint action  $\mathbf{a}_\tau$ ,  $r : \mathcal{X} \times \mathcal{U} \rightarrow [r_{\min}, r_{\max}]$  is a reward function encoding the objectives of the multi-robot task, and  $\gamma \in (0, 1)$  is the discount factor. Whereas the robot dynamics are formulated in continuous time, the MDP is formulated in discrete time based on the zero-order hold discretization in Eq. (2). Accordingly,  $p(\mathbf{s}_{\tau+1}|\mathbf{s}_\tau, \mathbf{a}_\tau)$  is a Gaussian density with mean  $\mathbf{s}_\tau + T\mathbf{f}(\mathbf{s}_\tau, \mathbf{a}_\tau)$  and covariance  $T\Xi$ .

The robots interact in a distributed manner, described by a time-varying undirected graph  $\mathcal{G}_\tau = (\mathcal{V}, \mathcal{E}_\tau)$ , where  $\mathcal{E}_\tau \subseteq \mathcal{V} \times \mathcal{V}$  is the set of edges. An edge  $(i, j) \in \mathcal{E}_\tau$  exists when robots  $i$  and  $j$  interact at time  $\tau$ . Let  $\mathbf{A}_\tau \in \{0, 1\}^{n \times n}$  be the adjacency matrix associated to  $\mathcal{G}_\tau$ , such that  $[\mathbf{A}_\tau]_{ij} = 1$  if and only if  $(i, j) \in \mathcal{E}_\tau$ , and 0 otherwise. The set of  $k$ -hop neighbors of robot  $i$  at time  $\tau$  is  $\mathcal{N}_\tau^{i,k} = \{j \in \mathcal{V} \mid [\mathbf{A}_\tau^k]_{ij} \neq 0\}$ . We remark that  $\mathcal{N}_\tau^{i,k}$  includes robot  $i$ .

The goal of this work is to learn distributed control policies that solve a given multi-robot task, such that they respect the networked structure of the multi-robot team and the MDP model. We represent the policies as stochastic Markov control policies that depend on the  $k$ -hop neighbors of robot  $i$ :

$$\mathbf{a}_\tau^i \sim \pi_\theta \left( \mathbf{a}_\tau^i | \mathbf{s}_{\mathcal{N}_\tau^{i,k}}^i \right). \quad (3)$$

Here,  $\mathbf{s}_{\mathcal{N}_\tau^{i,k}}^i = \{\mathbf{s}_\tau^j | j \in \mathcal{N}_\tau^{i,k}\}$  denotes the states of robot  $i$  and its  $k$ -hop neighbors, and  $\theta$  denotes the control policy parameters. The use of a stochastic Markov policy is not only motivated by the MDP model but also by the fact that distributed control policies are prone to uncertainty from the communication-perception modules, control goals, and interaction with the environment. We assume that the policy in Eq. (3) is the same for all the robots. The joint control policy of all the robots is denoted by  $\Pi_\theta = [\pi_\theta^\top(\mathbf{a}_\tau^1 | \mathbf{s}_{\mathcal{N}_\tau^{1,k}}^1), \dots, \pi_\theta^\top(\mathbf{a}_\tau^n | \mathbf{s}_{\mathcal{N}_\tau^{n,k}}^n)]^\top$ .

Learning a distributed control policy  $\pi_\theta$  that solves a certain multi-robot task is equivalently posed as learning the parameters  $\theta$  such that  $\pi_\theta$  maximizes the expected sum of

rewards over time, i.e.,

$$\begin{aligned} \max_{\theta} Q_{\Pi_{\theta}}(\mathbf{s}, \mathbf{a}) = \\ \max_{\theta} \mathbb{E}_{\mathbf{s}_{\tau} \sim p} \mathbb{E}_{\mathbf{a}_{\tau} \sim \Pi_{\theta}(\cdot | \mathbf{s}_{\tau})} \left[ \sum_{\tau=0}^{\infty} \gamma^{\tau} r(\mathbf{s}_{\tau}, \mathbf{a}_{\tau}) | \mathbf{s}_0 = \mathbf{s}, \mathbf{a}_0 = \mathbf{a} \right]. \end{aligned} \quad (4)$$

In Eq. (4), the function  $Q_{\Pi_{\theta}}(\mathbf{s}, \mathbf{a})$  is known as the action-value ( $Q$ ) function associated with the policy  $\Pi_{\theta}$  [46].

We do not make any assumptions on the reward function or action-value function, such as a specific factorization [14], [33]. The purpose of this work is to design a control policy that maximizes  $Q_{\Pi_{\theta}}(\mathbf{s}, \mathbf{a})$  and enforces the distributed factorization expressed in Eq. (3).

#### IV. PHYSICS-INFORMED MULTI-AGENT REINFORCEMENT LEARNING

In this section, we present a novel physics-informed multi-agent reinforcement learning approach to find distributed control policies that solve multi-robot tasks as defined in Eq. (4), under the restrictions on the robot dynamics and available information defined in Eq. (3). Our formulation is done in continuous time, following the continuous-time definition of the robot dynamics in Eq. (1). Later, zero-order hold control is used to utilize a discrete-time version of the control policies in the reinforcement learning algorithm.

First, we present a port-Hamiltonian formulation of the multi-robot dynamics and an energy-based distributed control design that can shape the interactions and the Hamiltonian of the closed-loop system (Sec. IV-A). Given experience from trial and error simulations, we employ a self-attention mechanism to learn the parameters of the control policy that maximize the cumulative reward (Sec. IV-B). To simplify the notation, we omit the time dependence of the states  $\mathbf{x}$  and controls  $\mathbf{u}$  in the remainder of the paper. To facilitate the exposition, in Sec. IV-A and IV-B we assume that the robot dynamics and control policies are deterministic. In Sec. V, we explain how to return to the stochastic setting.

##### A. Port-Hamiltonian dynamics for multi-robot energy conservation

Port-Hamiltonian mechanics are a general yet interpretable modeling approach for learning and control. On the one hand, many physical networked systems can be described as a port-Hamiltonian system [67] using the same formulation and with a modular and distributed interpretation. Meanwhile, the port-Hamiltonian description allows to derive general energy-based controllers with closed-loop stability guarantees. Since robots are physical systems that satisfy Hamiltonian mechanics, we model each robot as a port-Hamiltonian system [66]:

$$\dot{\mathbf{x}}^i = (\mathbf{J}^i(\mathbf{x}^i) - \mathbf{R}^i(\mathbf{x}^i)) \frac{\partial H^i(\mathbf{x}^i)}{\partial \mathbf{x}^i} + \mathbf{F}^i(\mathbf{x}^i) \mathbf{u}^i, \quad (5)$$

where the skew-symmetric interconnection matrix  $\mathbf{J}^i(\mathbf{x}^i)$  represents energy exchange within a robot, the positive-semidefinite dissipation matrix  $\mathbf{R}^i(\mathbf{x}^i)$  represents energy dissipation, the Hamiltonian  $H^i(\mathbf{x}^i)$  represents the total energy, and the matrix  $\mathbf{F}^i(\mathbf{x}_i)$  is the input gain.

The interconnection of port-Hamiltonian systems leads to another port-Hamiltonian system [71]. Therefore, if the control and state of each robot are considered as input and output energy ports, then, due to the modularity of port-Hamiltonian dynamics, the multi-robot system with joint state  $\mathbf{x}$  also follows port-Hamiltonian dynamics:

$$\dot{\mathbf{x}} = (\mathbf{J}(\mathbf{x}) - \mathbf{R}(\mathbf{x})) \frac{\partial H(\mathbf{x})}{\partial \mathbf{x}} + \mathbf{F}(\mathbf{x}) \mathbf{u}, \quad (6)$$

where  $\mathbf{J}(\mathbf{x})$ ,  $\mathbf{R}(\mathbf{x})$ , and  $\mathbf{F}(\mathbf{x})$  are block-diagonal:

$$\begin{aligned} \mathbf{J}(\mathbf{x}) &= \text{diag}(\mathbf{J}^1(\mathbf{x}^1), \dots, \mathbf{J}^n(\mathbf{x}^n)), \\ \mathbf{R}(\mathbf{x}) &= \text{diag}(\mathbf{R}^1(\mathbf{x}^1), \dots, \mathbf{R}^n(\mathbf{x}^n)), \\ \mathbf{F}(\mathbf{x}) &= \text{diag}(\mathbf{F}^1(\mathbf{x}^1), \dots, \mathbf{F}^n(\mathbf{x}^n)), \end{aligned} \quad (7)$$

and  $H(\mathbf{x}) = \sum_{i=1}^n H^i(\mathbf{x}^i)$ . It is noteworthy that the expression in Eq. (6) is control-affine and follows the definition of Eq. (1), with  $\mathbf{f}(\mathbf{x}, \mathbf{u}) = \mathbf{h}(\mathbf{x}) + \mathbf{g}(\mathbf{x}) \mathbf{u}$ ,  $\mathbf{h}(\mathbf{x}) = (\mathbf{J}(\mathbf{x}) - \mathbf{R}(\mathbf{x})) \frac{\partial H(\mathbf{x})}{\partial \mathbf{x}}$ ,  $\mathbf{g}(\mathbf{x}) = \mathbf{F}(\mathbf{x})$ , and  $\mathbf{L} = \mathbf{0}$  since we are considering a deterministic setting for now.

Without control, the trajectories of the open-loop system in (6) would follow the dynamics of the robots in the absence of interactions with the environment or other robots. The dynamics need to be controlled by a policy in order to accomplish the desired task. We propose to design a control policy  $\mu_{\theta}(\mathbf{x})$  and, then, obtain the desired policy in Eq. (3). Policy  $\mu_{\theta}(\mathbf{x})$  is designed using an Interconnection and Damping Assignment Passivity-Based Control (IDA-PBC) approach [66], which injects additional energy in the system through the control input  $\mathbf{u}$  to obtain closed-loop dynamics that achieve the desired task:

$$\dot{\mathbf{x}} = (\mathbf{J}_{\theta}(\mathbf{x}) - \mathbf{R}_{\theta}(\mathbf{x})) \frac{\partial H_{\theta}(\mathbf{x})}{\partial \mathbf{x}}, \quad (8)$$

with Hamiltonian  $H_{\theta}(\mathbf{x})$ , skew-symmetric interconnection matrix  $\mathbf{J}_{\theta}(\mathbf{x})$ , and positive semidefinite dissipation matrix  $\mathbf{R}_{\theta}(\mathbf{x})$ , which depend on the control policy  $\mu_{\theta}(\mathbf{x})$ . By matching the terms in (6) and (8), one obtains the joint policy:

$$\begin{aligned} \mathbf{u} &= \Pi_{\theta}(\mathbf{x}) = \\ \mathbf{F}^{\dagger}(\mathbf{x}) &\left( (\mathbf{J}_{\theta}(\mathbf{x}) - \mathbf{R}_{\theta}(\mathbf{x})) \frac{\partial H_{\theta}(\mathbf{x})}{\partial \mathbf{x}} - (\mathbf{J}(\mathbf{x}) - \mathbf{R}(\mathbf{x})) \frac{\partial H(\mathbf{x})}{\partial \mathbf{x}} \right), \end{aligned} \quad (9)$$

where  $\mathbf{F}^{\dagger}(\mathbf{x}) = (\mathbf{F}^{\top}(\mathbf{x}) \mathbf{F}(\mathbf{x}))^{-1} \mathbf{F}^{\top}(\mathbf{x})$  is the pseudo-inverse of  $\mathbf{F}(\mathbf{x})$ .

If the robots are fully-actuated, i.e.,  $\mathbf{F}(\mathbf{x})$  is full-rank, then the input  $\mathbf{u}$  in (9) exactly transforms the open loop system in (6) to the closed-loop system in (8). For underactuated systems, the transformation may not be exact [72]. Being able to maximize  $Q_{\Pi_{\theta}}$  is, hence, related to whether the robot configurations that solve the task are realizable by the class of control policies in (9). Even if goals of the task are not realizable, the policy parameters  $\theta$  may still be optimized to achieve a behavior as good as possible to solve the task.

Let  $[\mathbf{J}_{\theta}(\mathbf{x})]_{ij}$  and  $[\mathbf{R}_{\theta}(\mathbf{x})]_{ij}$  denote the  $n_x \times n_x$  blocks with index  $(i, j)$ , representing the energy exchange between robot  $i$  and  $j$  and the energy dissipation of robot  $i$  caused

by robot  $j$ , respectively. Since the input gain  $\mathbf{F}(\mathbf{x})$  in (7) is block-diagonal, the individual control policy of robot  $i$  is:

$$\mu_{\theta}(\mathbf{x}) = (\mathbf{F}^i)^{\dagger}(\mathbf{x}^i) \left( \sum_{j \in \mathcal{V}} ([\mathbf{J}_{\theta}(\mathbf{x})]_{ij} - [\mathbf{R}_{\theta}(\mathbf{x})]_{ij}) \frac{\partial H_{\theta}(\mathbf{x})}{\partial \mathbf{x}_j} - (\mathbf{J}^i(\mathbf{x}^i) - \mathbf{R}^i(\mathbf{x}^i)) \frac{\partial H^i(\mathbf{x})}{\partial \mathbf{x}^i} \right). \quad (10)$$

Note that the individual control policy  $\mu_{\theta}(\mathbf{x})$  in (10) does not necessarily respect the hops in the communication network as desired in (3) because it depends on the structure of  $\mathbf{J}_{\theta}(\mathbf{x})$ ,  $\mathbf{R}_{\theta}(\mathbf{x})$ , and  $H_{\theta}(\mathbf{x})$ . In Sec. IV-B, we impose conditions on these terms to ensure that they respect the communication topology and are skew-symmetric, positive semidefinite and positive respectively, as required for a valid port-Hamiltonian system and to find a policy  $\mu_{\theta}$  that only depends on the  $k$ -hop neighbors.

### B. Self-attention parameterization to enforce communication patterns

We seek to learn distributed control policies that follow the structure of Eqs. (9)-(10) and (i) scale with the number of robots, (ii) handle time-varying communication and (iii) guarantee the port-Hamiltonian constraints. To do so, we first derive conditions on the port-Hamiltonian terms of the controller,  $\mathbf{J}_{\theta}(\mathbf{x})$ ,  $\mathbf{R}_{\theta}(\mathbf{x})$  and  $H_{\theta}(\mathbf{x})$ , which are the terms to be learned from the reinforcement learning experience. Then, we develop a novel architecture based on self-attention to ensure that the learned control policies guarantee the desired requirements. We summarize the overall neural network architecture in Fig. 2.

To respect the robot team topology defined by the graph  $\mathcal{G}$ , we first impose  $\mathbf{J}_{\theta}(\mathbf{x})$  and  $\mathbf{R}_{\theta}(\mathbf{x})$  to be block-sparse,

$$[\mathbf{J}_{\theta}(\mathbf{x})]_{ij} = [\mathbf{R}_{\theta}(\mathbf{x})]_{ij} = \mathbf{0}, \quad \forall j \notin \mathcal{N}^{i,k}. \quad (11)$$

From the perspective of robot  $i$ , this means that the controller only considers information from its  $k$ -hop neighbors. Moreover, we require that the desired Hamiltonian factorizes over the  $k$ -hop neighborhoods:

$$H_{\theta}(\mathbf{x}) = \sum_{i=0}^n H_{\theta}^i(\mathbf{x}_{\mathcal{N}^{i,k}}^i), \quad (12)$$

with  $\mathbf{x}_{\mathcal{N}^{i,k}}^i = \{\mathbf{x}^j | j \in \mathcal{N}^{i,k}\}$ . The factorization in (12) ensures that each robot  $i$  can calculate

$$\frac{\partial H_{\theta}(\mathbf{x})}{\partial \mathbf{x}^i} = \sum_{j \in \mathcal{N}^{i,k}} \frac{\partial H_{\theta}^j(\mathbf{x}_{\mathcal{N}^{j,k}}^j)}{\partial \mathbf{x}^i} \quad (13)$$

by gathering  $\partial H_{\theta}^j(\mathbf{x}_{\mathcal{N}^{j,k}}^j)/\partial \mathbf{x}^i$  from its  $k$ -hop neighbors. Then, the control policy  $\mu_{\theta}$  of robot  $i$  becomes:

$$\mu_{\theta}(\mathbf{x}) = (\mathbf{F}^i(\mathbf{x}^i))^{\dagger} \left( \sum_{j \in \mathcal{N}^{i,k}} ([\mathbf{J}_{\theta}(\mathbf{x})]_{ij} - [\mathbf{R}_{\theta}(\mathbf{x})]_{ij}) \frac{\partial H_{\theta}(\mathbf{x})}{\partial \mathbf{x}_j} - (\mathbf{J}^i(\mathbf{x}^i) - \mathbf{R}^i(\mathbf{x}^i)) \frac{\partial H^i(\mathbf{x})}{\partial \mathbf{x}^i} \right). \quad (14)$$

Imposing the requirements in (11)-(12) is a first step towards making the control policy in (14) distributed. Note that the

terms  $[\mathbf{J}_{\theta}(\mathbf{x})]_{ij}$  and  $[\mathbf{R}_{\theta}(\mathbf{x})]_{ij}$  might still depend on the joint state vector  $\mathbf{x}$  even though the sum runs over the  $k$ -hop neighbors in  $\mathcal{N}^{i,k}$ . Next, we discuss how to remove this dependence and achieve a similar factorization as (12).

First, we model  $[\mathbf{J}_{\theta}(\mathbf{x})]_{ij}$ ,  $[\mathbf{R}_{\theta}(\mathbf{x})]_{ij}$ , and  $H_{\theta}^i(\mathbf{x})$  in Eq. (14) with the parameters  $\theta$  shared across the robots, so that the team can handle time-varying communication graphs. Specifically, we propose a novel architecture based on self-attention [70]. Self-attention layers extract the relationships among the inputs of a sequence by calculating the importance associated to each input using an attention map. The length of the sequences can vary as the number of parameters of the self-attention is constant with the number of inputs. Our key idea is to consider the self and neighboring states as the sequence, where each neighbor's state is an input. We now detail how to model each of the port-Hamiltonian terms.

To learn  $[\mathbf{R}_{\theta}(\mathbf{x})]_{ij}$ , robot  $i$  will use, at instant  $t$ , the state  $\mathbf{x}^j$  from all  $k$ -hop neighbors  $j \in \mathcal{N}^{i,k}$ . The sequence of states is given by  $\mathbf{x}_{\mathcal{N}^{i,k}}^i$ . The proposed architecture is composed by a sequence of layers, indexed using the subscript  $w = 1, \dots, W$ . Following a self-attention mechanism, each layer computes the operations presented below:

$$\begin{aligned} \mathbf{Q}_1^i &= \mathbf{A}_1^{\mathbf{R}} \mathbf{x}_{\mathcal{N}^{i,k}}^i, \quad \mathbf{K}_1^i = \mathbf{B}_1^{\mathbf{R}} \mathbf{x}_{\mathcal{N}^{i,k}}^i, \quad \mathbf{V}_1^i = \mathbf{C}_1^{\mathbf{R}} \mathbf{x}_{\mathcal{N}^{i,k}}^i \\ \mathbf{Y}_1^i &= \chi \left( \text{softmax} \left( \frac{\beta(\mathbf{Q}_1^i) \beta((\mathbf{K}_1^i)^{\top})}{\sqrt{|\mathcal{N}^{i,k}|}} \right) \beta(\mathbf{V}_1^i) \right), \\ \mathbf{X}_1^i &= \psi(\mathbf{D}_1^{\mathbf{R}} \mathbf{Y}_1^i), \\ &\vdots \\ \mathbf{Q}_w^i &= \mathbf{A}_w^{\mathbf{R}} \mathbf{X}_{w-1}^i, \quad \mathbf{K}_w^i = \mathbf{B}_w^{\mathbf{R}} \mathbf{X}_{w-1}^i, \quad \mathbf{V}_w^i = \mathbf{C}_w^{\mathbf{R}} \mathbf{X}_{w-1}^i \\ \mathbf{Y}_w^i &= \chi \left( \text{softmax} \left( \frac{\beta(\mathbf{Q}_w^i) \beta((\mathbf{K}_w^i)^{\top})}{\sqrt{|\mathcal{N}^{i,k}|}} \right) \beta(\mathbf{V}_w^i) \right), \\ \mathbf{X}_w^i &= \psi(\mathbf{D}_w^{\mathbf{R}} \mathbf{Y}_w^i), \end{aligned} \quad (15)$$

where  $\beta(\cdot)$ ,  $\chi(\cdot)$ , and  $\psi(\cdot)$  are nonlinear activation functions. In the aforementioned operations,  $\mathbf{A}_w^{\mathbf{R}}, \mathbf{B}_w^{\mathbf{R}}, \mathbf{C}_w^{\mathbf{R}} \in \mathbb{R}^{r_w \times h_w}$  and  $\mathbf{D}_w^{\mathbf{R}} \in \mathbb{R}^{n_x \times r_w}$  for  $w = 1, \dots, W$  are matrices to be learned and shared across robots; and  $h_w, r_w, d_w > 0$ , with  $d_w = n_x$  and  $h_1 = n_x$  for valid matrix multiplications. Matrices  $\mathbf{A}_w^{\mathbf{R}}, \mathbf{B}_w^{\mathbf{R}}, \mathbf{C}_w^{\mathbf{R}}$  are of fixed size, so they are independent of the number of robots and neighbors. Thus, robot  $i$  can deal with time-varying neighbors. In particular,  $\mathbf{A}_1^{\mathbf{R}}, \mathbf{B}_1^{\mathbf{R}}, \mathbf{C}_1^{\mathbf{R}}$  transforms the states to features encoded in the query  $\mathbf{Q}_1^i$ , key  $\mathbf{K}_1^i$  and value  $\mathbf{V}_1^i$  matrices. Then,  $[\mathbf{R}_{\theta}(\mathbf{x})]_{ij}$  is constructed as a weighted matrix that models the interactions of robot  $i$  with its  $k$ -hop neighbors, and a diagonal positive semidefinite matrix that accounts for the self-interactions:

$$\begin{aligned} \mathbf{Z}_{ij}^{\mathbf{R}} &= \text{diag}(\mathbf{x}_W^{i,j}), \\ [\mathbf{R}_{\theta}(\mathbf{x})]_{ij} &= -(\mathbf{Z}_{ij}^{\mathbf{R}} + \mathbf{Z}_{ji}^{\mathbf{R}}), \quad \forall j \in \mathcal{N}^{i,k}, \\ [\mathbf{R}_{\theta}(\mathbf{x})]_{ii} &= \mathbf{Z}_{ii}^{\mathbf{R}} + \sum_{j \in \mathcal{N}^{i,k}} (\mathbf{Z}_{ij}^{\mathbf{R}} + \mathbf{Z}_{ji}^{\mathbf{R}}), \end{aligned} \quad (16)$$

where  $\mathbf{x}_W^{i,j}$  is the column that corresponds to neighbor  $j$  in  $\mathbf{X}_W^i$ , and  $\text{diag}(\cdot)$  is the operator that reshapes the  $n_x \times 1$  vector to a  $n_x \times n_x$  diagonal matrix. If the nonlinear activation function  $\psi(\cdot)$  is designed such that the elements of the output

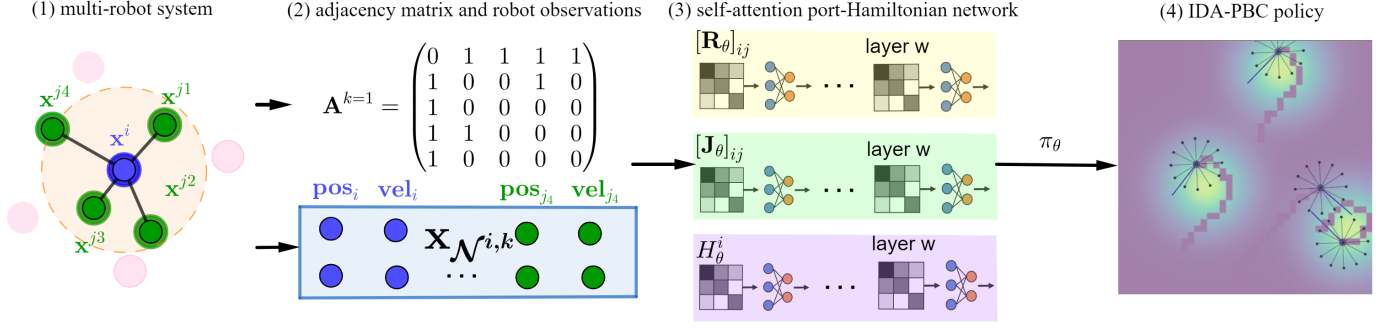


Fig. 2. Physics-informed neural network. Robot  $i$  receives information from the state of its  $k$ -hop neighbors. Then, each self-attention-based module process the data to obtain the port-Hamiltonian terms of the controller. Finally, robot  $i$  uses the learned IDA-PBC policy to compute the control input.

$\mathbf{X}_W^i$  are positive, then  $\mathbf{Z}_{ij}^{\mathbf{R}}$  is a diagonal positive semidefinite matrix and  $\mathbf{R}_\theta(\mathbf{x})$  is a diagonally dominant matrix. This way,  $\mathbf{R}_\theta(\mathbf{x})$  is positive semidefinite by design. In fact, note the similarities between (16) and a weighted Laplacian matrix. More importantly, each element  $[\mathbf{R}_\theta(\mathbf{x})]_{ij}$  depends only on the information from robot  $i$  and its neighbor  $j$ , so the computation is distributed.

To learn  $[\mathbf{J}_\theta(\mathbf{x})]_{ij}$ , we follow the same steps in (15), with parameters  $\mathbf{A}_w^{\mathbf{J}}, \mathbf{B}_w^{\mathbf{J}}, \mathbf{C}_w^{\mathbf{J}}, \mathbf{D}_w^{\mathbf{J}}$  instead of  $\mathbf{A}_w^{\mathbf{R}}, \mathbf{B}_w^{\mathbf{R}}, \mathbf{C}_w^{\mathbf{R}}, \mathbf{D}_w^{\mathbf{R}}$ , to obtain encodings  $\mathbf{Z}_{ij}^{\mathbf{J}}$  instead of  $\mathbf{Z}_{ij}^{\mathbf{R}}$ . Due to the reciprocal communication between robots  $i$  and  $j$ , we enforce the skew-symmetry of  $\mathbf{J}_\theta(\mathbf{x})$  by:

$$[\mathbf{J}_\theta(\mathbf{x})]_{ij} = \mathbf{Z}_{ij}^{\mathbf{J}} - \mathbf{Z}_{ji}^{\mathbf{J}} \quad \forall j \in \mathcal{N}^{i,k}. \quad (17)$$

Since  $[\mathbf{J}_\theta(\mathbf{x})]_{ij} = 0$ , the interconnection matrix is such that  $\mathbf{J}_\theta(\mathbf{x}) + \mathbf{J}_\theta^\top(\mathbf{x}) = \mathbf{0}$  and, thus, is skew-symmetric by design. Again, each element  $[\mathbf{J}_\theta(\mathbf{x})]_{ij}$  depends only on the information from robot  $i$  and its neighbor  $j$ , so the computation is distributed.

Finally, to learn  $H_\theta^i(\mathbf{x}_{\mathcal{N}^{i,k}}^i)$ , we represent it as follows:

$$H_\theta^i(\mathbf{x}_{\mathcal{N}^{i,k}}^i) = \text{vec}(\mathbf{x}_{\mathcal{N}^{i,k}}^i)^\top \mathbf{M}_\theta^i(\mathbf{x}_{\mathcal{N}^{i,k}}^i) \text{vec}(\mathbf{x}_{\mathcal{N}^{i,k}}^i) + U_\theta^i(\mathbf{x}_{\mathcal{N}^{i,k}}^i). \quad (18)$$

The first term in the right-hand side of Eq. (18) is a kinetic-like energy function and the second terms is a potential energy function with

$$\mathbf{M}_\theta^i(\mathbf{x}_{\mathcal{N}^{i,k}}^i) = \text{diag}(\mathbf{1}^\top \mathbf{Z}_i^{\mathbf{M}}) \text{ and } U_\theta^i(\mathbf{x}_{\mathcal{N}^{i,k}}^i) = \mathbf{1}^\top \mathbf{Z}_i^{\mathbf{U}} \mathbf{1}.$$

The encodings  $\mathbf{Z}_i^{\mathbf{M}}$  and  $\mathbf{Z}_i^{\mathbf{U}}$  are calculated using the same steps in (15), with parameters  $\mathbf{A}_w^{\mathbf{M}}, \mathbf{B}_w^{\mathbf{M}}, \mathbf{C}_w^{\mathbf{M}}, \mathbf{D}_w^{\mathbf{M}}$  and  $\mathbf{A}_w^{\mathbf{U}}, \mathbf{B}_w^{\mathbf{U}}, \mathbf{C}_w^{\mathbf{U}}, \mathbf{D}_w^{\mathbf{U}}$ , respectively. Once we have  $H_\theta^j(\mathbf{x}_{\mathcal{N}^{j,k}}^j)$ , we obtain  $\partial H_\theta^j(\mathbf{x}_{\mathcal{N}^{j,k}}^j)/\partial \mathbf{x}^j$  from all the neighboring robots and compute Eq. (13). Therefore, since all the operations are only dependent on the available information in robot  $i$  and its neighbor  $j$ , the computations involving the Hamiltonian function are distributed by design.

To deploy the control policy (14), we design a message  $\mathbf{m}_{\tau,j}^{i,j}$ , encoding information that robot  $i$  needs from robot  $j$  at time  $\tau$  to calculate  $[\mathbf{J}_\theta(\mathbf{x})]_{ij}$ ,  $[\mathbf{R}_\theta(\mathbf{x})]_{ij}$ , and  $H_\theta^i(\mathbf{x})$ . When there is no communication among robots, i.e.,  $k = 0$ , no message is needed. For  $k \geq 1$ , robot  $i$  uses the following communication protocol:

- 1) Robot  $i$  receives messages  $\mathbf{m}_{\tau,1}^{i,j} = \mathbf{x}_j$  from its  $k$ -hop neighbors in  $\mathcal{N}^{i,k}$ . Then, robot  $i$  computes  $\mathbf{Z}_{ij}^{\mathbf{R}}, \mathbf{Z}_{ij}^{\mathbf{J}}, H_\theta^i$ , and  $\partial H_\theta^i/\partial \mathbf{x}_j$ .
- 2) Robot  $i$  receives messages  $\mathbf{m}_{\tau,2}^{i,j} = \{\partial H_\theta^j/\partial \mathbf{x}_i, \mathbf{Z}_{ji}^{\mathbf{R}}, \mathbf{Z}_{ji}^{\mathbf{J}}\}$  from its  $k$ -hop neighbors in  $\mathcal{N}^{i,k}$  and computes  $\partial H_\theta/\partial \mathbf{x}_i, [\mathbf{J}_\theta]_{ij}, [\mathbf{R}_\theta]_{ij}$ .
- 3) Robot  $i$  receives messages  $\mathbf{m}_{\tau,3}^{i,j} = \partial H_\theta/\partial \mathbf{x}_j$  from its  $k$ -hop neighbors in  $\mathcal{N}^{i,k}$  and computes the control input  $\mathbf{a}_i$ .

In summary, each robot  $i$  receives a message  $\mathbf{m}_{\tau,j}^{i,j} = [\mathbf{m}_{\tau,1}^{i,j}, \mathbf{m}_{\tau,2}^{i,j}, \mathbf{m}_{\tau,3}^{i,j}]$  in 3 communication rounds from its neighboring robot  $j$ . We assume negligible delays between communication rounds. If the delay is large, Wang et al. [60] suggest to learn a function that predicts quantities such as  $\partial H_\theta(\mathbf{x})/\partial \mathbf{x}_j, \mathbf{Z}_{ji}^{\mathbf{J}}, \mathbf{Z}_{ji}^{\mathbf{R}}$ , leading to one communication round. We leave this for future work.

## V. PHYSICS-INFORMED MULTI-ROBOT SOFT ACTOR-CRITIC

The previous section describes how to parameterize the distributed control policies to be learned. In this section, we present a soft actor-critic algorithm [73] to train the self-attention port-Hamiltonian neural network, detailing the main features that allow the integration of our physics-informed policy representation. The key components are presented in Fig. 3, namely: (a) actor, (b) environment, (c) reward, and (d) critic.

### A. The actor

First, we model the actor with the port-Hamiltonian system detailed in Sec. IV-A and we use the IDA-PBC policy in Eq. (14) parameterized by the self-attention architecture proposed in Sec. IV-B. The known robot dynamics are typically provided by the simulation environments or the hardware specifications of the robots [74]. Nevertheless, two aspects must be adapted to match the soft actor-critic formulation: (i) the MDP formulation and the stochastic Markov policy are in discrete time while the robot dynamics and the IDA-PBC are in continuous-time, and (ii) the actions in the soft actor-critic method are stochastic while the port-Hamiltonian formulation is deterministic.



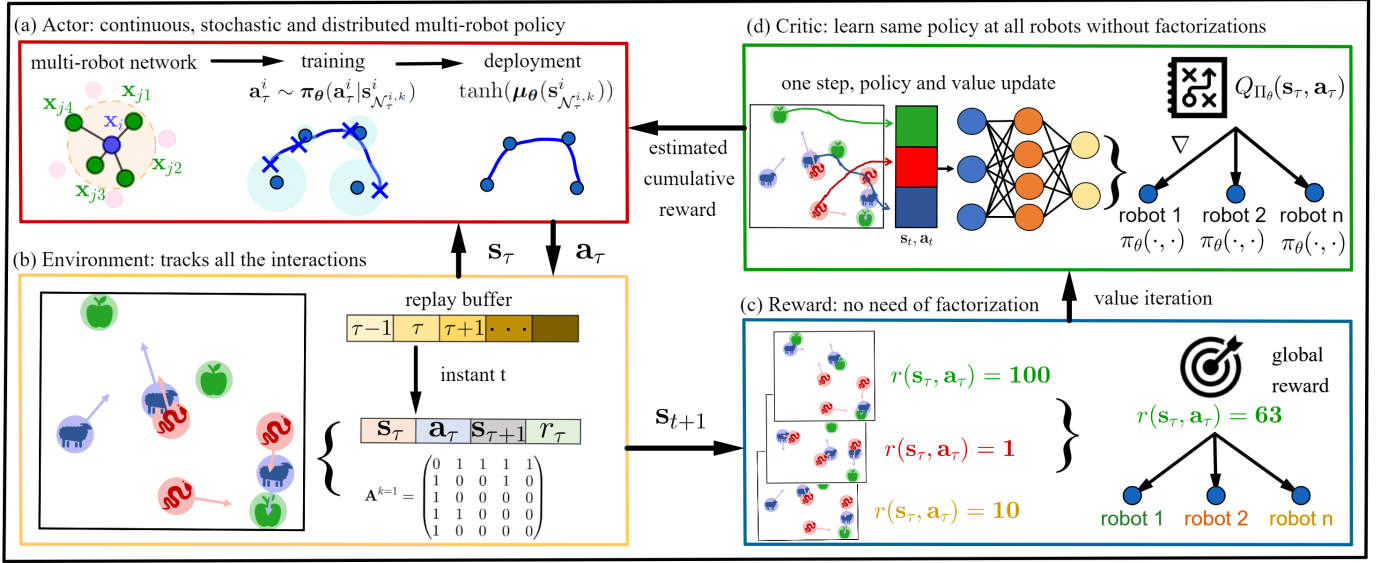


Fig. 3. Overview of our physics-informed multi-agent reinforcement learning approach. The soft actor-critic method consists of: (a) an actor, the IDA-PBC self-attention-based neural network policy, (b) an interactive environment with, e.g., goals to reach and adversaries to avoid, and that keeps track of the correlations among robots encoded in the communication graph, (c) a global reward function that describes the task and steers the multi-agent reinforcement learning training without any particular factorization, and (d) a centralized critic, modeled as a neural network that learns the state-action value function relating the agent and the environment according to the desired task, which allows to learn the same policy for all the robots simultaneously with the same policy and value updates.

To address the continuous versus discrete time mismatch, we use the zero-order hold control approach described in Sec. III. More specifically,  $\mathbf{u}(t) = \mathbf{a}_\tau = \mu_\theta(\mathbf{x}(t_\tau))$  for  $t \in [t_\tau, t_{\tau+1})$ . This means that we can write the control policy as dependent on the discrete-time state  $\mathbf{s}_\tau$  rather than the continuous-time state  $\mathbf{x}(t_\tau)$ , leading to  $\mu_\theta(\mathbf{s}_\tau)$  with the same expression in Eq. (14).

To address stochasticity and maintain the desired distributed structure already derived in Sec. IV-A and IV-B, we model the distributed control policies as (squashed) Gaussian distributions, whose mean is given by the IDA-PBC controller in (14), therefore respecting the distributed policy factorization. Meanwhile, the variance of the policy distribution is provided by a neural network that is learned during training. Overall, we obtain a distributed and stochastic Markov control policy of the form:

$$\mathbf{a}_\tau^i \sim \pi_\theta(\mathbf{a}_\tau^i | \mathbf{s}_{\mathcal{N}_\tau^i, k}^i) = \tanh(\mu_\theta(\mathbf{s}_{\mathcal{N}_\tau^i, k}^i) + \sigma_\psi(\mathbf{a}_\tau^i, \mathbf{s}_{\mathcal{N}_\tau^i, k}^i)\xi), \quad (19)$$

where  $\mu_\theta(\mathbf{s}_{\mathcal{N}_\tau^i, k}^i)$  is the IDA-PBC policy parameterized by self-attention neural networks under the restrictions imposed by the networked structure of the robot team. On the other hand,  $\sigma_\psi(\mathbf{a}_\tau^i, \mathbf{s}_{\mathcal{N}_\tau^i, k}^i)$  is a vector of standard deviations given by a neural network that approximates the variance of the squashed Gaussian distribution with parameters  $\psi$ . Besides,  $\xi \sim \mathcal{N}(\mathbf{0}, \mathbf{I})$ , so the control policy is a Gaussian distribution with mean  $\mu_\theta(\mathbf{s}_{\mathcal{N}_\tau^i, k}^i)$  and diagonal covariance matrix whose diagonal is equal to  $(\sigma_\psi(\mathbf{a}_\tau^i, \mathbf{s}_{\mathcal{N}_\tau^i, k}^i))^2$ . The control is constrained to  $\mathbf{a}_\tau^i \in [-1, 1]^{n_u}$  by means of a tanh function [54], [73], [75], leading to a squashed Gaussian policy. In practice, the control input can be constrained to  $\mathbf{a}_\tau^i \in [a_{\min}, a_{\max}]^{n_u}$  with  $-\infty < a_{\min} \leq a_{\max} < \infty$  by scaling the output

of the tanh function. It is also important to remark that  $\sigma_\psi(\mathbf{a}_\tau^i, \mathbf{s}_{\mathcal{N}_\tau^i, k}^i)$  only depends on the available information at each robot, such that the desired distributed factorization of the control policy is preserved.

During training, the control inputs are sampled from the Gaussian distribution, as stated in Eq. (3). After training, the mean control input is chosen, i.e.,  $\mathbf{a}_\tau^i = \tanh(\mu_\theta(\mathbf{s}_{\mathcal{N}_\tau^i, k}^i))$ . In the case that an additional layer of robust, adaptive or active control is desired, then  $\sigma_\psi(\mathbf{a}_\tau^i, \mathbf{s}_{\mathcal{N}_\tau^i, k}^i)$  can be used as a proxy of the uncertainty in the control policy, since it only depends on the neighboring information at robot  $i$ . The design of  $\sigma_\psi(\mathbf{a}_\tau^i, \mathbf{s}_{\mathcal{N}_\tau^i, k}^i)$  is free to choose, but in this work we opt for the same architecture in Eq. (15).

### B. The environment

The second modification over the soft actor-critic algorithm is in the collection of experience from the environment. The environment is determined by the desired task to be solved, with examples found in Fig. 1. The main difference with other multi-agent reinforcement learning works is that, to build the replay buffer that stores the trial and error experience used for training the control policies, we take into account all the interactions among the robots. Differently from centralized-training decentralized-deployment approaches, where the experience of each agent is recorded independently of the other agents, we record for each experience all the robot states, actions, and interaction graph together. Thanks to that, we keep track of the correlation among robots during training. This also allows us to condition the trained control policies on the available information at each robot, therefore only providing the information robots will have access during deployment.

### C. The reward

The reward function can be shared across robots and include global terms because the actor is the whole multi-robot network. This is important because, from the perspective of the soft actor-critic algorithm during training, the whole robot network is a single centralized agent. Other state-of-the-art multi-agent reinforcement learning approaches (see Sec. II) require a factorization of the reward function because each agent is considered as an isolated learning unit which does not exploit neighboring information during the execution of the control policy. In contrast, in our approach the shared distributed control policy is simultaneously learned at all the robots used in training, and since the experience record the underlying communication graph, we can seamlessly associate global rewards with distributed cooperative control policies through communication. It is worth to note that, as in any classical soft actor-critic approach, the maximization objective is changed to include an entropy term  $\mathcal{H}(\Pi_\theta(\mathbf{a}|\mathbf{s}))$  that measures the entropy of the control policy. This entropy term, weighted by a temperature parameter  $\alpha > 0$ , trades off exploration (high value) and exploitation (low value). The value of  $\alpha$  changes over time according to a gradient descend law which manages automatically the exploration/exploitation dichotomy. The details of this automatic temperature adjustment rule can be found in [73].

### D. The critic

Finally, regarding the critic, its main purpose is to learn the action-value function of the environment, encoded in  $Q_{\Pi_\theta}(\mathbf{s}, \mathbf{a})$ . This approximation steers the training of the control policy towards the maximization objective. Nevertheless and importantly, the critic is only used during training. Thus, it is not necessary to design it to be distributed and an existing centralized neural network architecture can be used. In this work, we opt for a multi-layer perceptron with parameters  $\vartheta$  to learn  $Q_{\Pi_\theta}^\vartheta(\mathbf{s}, \mathbf{a})$ . As with the reward, since, from the perspective of the soft actor-critic algorithm, the single agent is the whole robot network described by the port-Hamiltonian dynamics, a single centralized critic can learn the appropriate action-value function to condition the training of the distributed control policy.

A shared centralized action value function implies that each optimization step considers, simultaneously, all the policies gathered in the joint policy  $\Pi_\theta$ . Since the policies are homogeneous, each optimization step is simultaneously updating the policy  $\pi_\theta$   $n$  times. This is achieved without any particular specification of the gradients nor factorization of the action value function. This is one of the key properties and advantages of our proposed soft actor-critic algorithm compared to other state-of-the-art algorithms. Typical multi-agent reinforcement learning approaches, by factorizing the policy and/or the value functions, arrive to a different set of policy parameters, one per agent used in training. In cooperative tasks where the robots share the same goal, there should be a single policy that resolves the task independently on the configuration of the robot. In our case, by appropriately integrating the modular port-Hamiltonian description of the

multi-robot system with the soft actor-critic algorithm, we train a single distributed control policy which takes into account the current available information at each robot. Using the soft actor-critic update rules [54], [73], [75], the gradients with respect to  $\theta$  are, simultaneously for all the robots, already conditioned on the multi-robot communication topology.

In conclusion, in contrast with other solutions, ours explicitly considers the exchanges of information among robots by modeling the multi-robot system as a graph. This allows to use a reinforcement learning algorithm for single-robot problems, where the single agent is the multi-robot network. From the perspective of the reinforcement learning algorithm, the actor is centralized. However, by means of a physics-informed self-attention parameterization of the dynamics and control of the robots, the learned policies are distributed by design, modeling the robot team as a modular port-Hamiltonian system.

## VI. RESULTS

To assess our physics-informed multi-agent reinforcement learning approach, we present six multi-robot scenarios. The first three are extracted from the VMAS simulator [74] and the last three are adaptations from the MPE simulator [57], [76] that can be found in [60]:

- a) **Reverse transport:** the robots are randomly spawned inside a box that they must push towards a desired landmark in the arena. The initial position of the box and the landmark is random. Compared to [74], we decrease the mass of the box to 1 kg to ensure that the box can be moved even with a small number of robots. Also, when the box is in the landmark, the reward is set to 1.
- b) **Sampling:** the robot team is randomly spawned in an arena with an underlying Gaussian density function composed of 3 modes. The field is discretized to a grid. Robots must collect samples of the field such that once a robot visits a cell its sample is collected without replacement and given as reward to the team. Robots use a LiDAR to sense each other, and they observe the samples in the  $3 \times 3$  grid around it.
- c) **Navigation:** each robot has a landmark to reach. The initial position of the robots and landmarks are randomly spawned in a  $2 \times 2$  m square arena. Robots must navigate to reach their corresponding landmarks while avoiding collisions with other robots. Compared to [74], we encourage collision avoidance by changing the collision penalty from  $-1$  to  $-5$ . Besides, each robot only observes its desired landmark instead of all the landmarks.
- d) **Food collection:** it is a version of the simple spread scenario [57] where a team of robots and food landmarks is randomly spawned in an arena. There are as many landmarks as robots. Robots must cooperate to cover as many food landmarks as possible. Each time a robot covers a new landmark, the whole team is rewarded.
- e) **Grassland:** A team of robots must collect food resources that are randomly spawned in an arena, while evading multiple predators. There are as many robots as predators, and the former move twice faster than the latter. The predator team is positively rewarded when some member



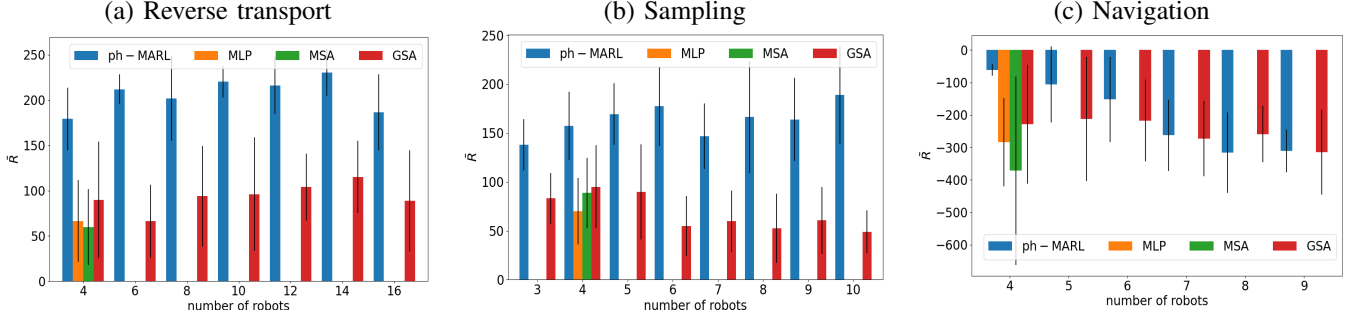


Fig. 4. Comparison of the performance of the ablated control policies when we scale the number of robots in deployment. In all the scenarios, our proposed combination of a port-Hamiltonian modeling and self-attention-based neural networks achieves the best cumulative reward without further training the control policy. Each bar displays the mean and standard deviation of  $\bar{R}$  over 10 evaluation episodes.

captures a robot, whereas the robot team is negatively rewarded and the robot is deactivated. On the other hand, the robots receive a positive reward if they reach a food landmark, which is then spawned again in a new position.

- f) **Adversarial**: two robotic teams compete for the same food landmarks. Both teams have the same number of robots. When a member of a team reaches a food landmark, the landmark is randomly spawned and the team is positively rewarded. When two members of a team collide with one member of the other team, then the first team is positively rewarded, while the second team is penalized and the robot deactivated.

The first three scenarios are used for ablation studies, while the other three are used to compare our method with other state-of-the-art approaches.

All robots have a communication radius  $r_{comm} > 0$  which allows to exchange information with 1-hop neighbors. The communication radius and other hyperparameters of the soft actor-critic algorithm are specified in Appendix B. Each robot observes its position, velocity, position and velocity of the landmarks or objects of interest (e.g., the box in reverse transport). The particularities of the observation space of each robot can be found in [57], [60], [74]. In some scenarios, the robot observation vector changes its dimension depending on the number of robots. Specifically, in the food collection, grassland and adversarial scenarios the number of landmarks changes with the number of robots. Therefore, to accommodate the proposed self-attention port-Hamiltonian neural network with an observation vector which may change its size, we use an additional neural network to pre-process the observation vector. In particular, we concatenate a self-attention layer with a dense layer which receives, as input, the food landmarks' positions and outputs a feature vector of constant dimension that is used as part of the state vector to build  $\mathbf{S}_t^i$ . The details can be found in Appendix A. Supplementary material can be found in our repository<sup>1</sup>.

#### A. Ablation results

We conduct ablation studies using the reverse transport, sampling and navigation scenarios. We compare the proposed self-attention port-Hamiltonian neural network (pH-MARL)

with a classical multi-layer perceptron (MLP), a modular self-attention-based neural network (MSA) and a graph- and attention-based neural network (GSA). The implementation details can be found in Appendix A.

The MLP network is an unstructured neural network that receives, as input, the current states and actions of the robots and outputs the action vector. The MSA network replaces the dense layers of the MLP network with an architecture based on self-attention, but has the same input and output. The GSA network is similar to the MSA network but has the adjacency matrix as additional input. The three neural networks constitute a sequential improvement from a standard neural network to our port-Hamiltonian formulation. It is important to note that, with the current formulation, it is not possible to try a port-Hamiltonian neural network which is not based on self-attention because each element of the processed input sequence is employed to compute the port-Hamiltonian terms, that are also a sequence spanned from  $i \in \mathcal{N}_t^{i,k}$ . This is key for the scalability of the policy and is a feature that is not provided by other architectures based on, e.g., multi-layer perceptrons or convolutions.

Finally, we employ the same architecture used in pH-MARL to learn the standard deviation for all the options, along with the same critic and soft actor-critic algorithm (Appendix A).

Table I shows the averaged cumulative reward  $\bar{R} = \frac{1}{n} R = \frac{1}{n} \sum_{\tau=0}^{\tau_{\max}-1} r(\mathbf{s}_\tau, \mathbf{a}_\tau)$  after convergence of the training, where  $\tau_{\max}$  is the maximum number of steps per episode. For the three scenarios and the four neural network architectures, we use  $n = 4$  robots. The table reports the mean of  $\bar{R}$  over 10 evaluation episodes. In all the cases, pH-MARL surpasses the other three architectures, with a particularly significant difference in the reverse transport and navigation scenarios. Given the same number of parameters in the four architectures, the use of a physics-informed formulation of the neural network leads to a structured learning with efficient sampling in training. The difference in the reverse transport scenario is due to the fact that the other networks sometimes fail in reaching the landmark, despite arriving to a very close position. In the sampling scenario, pH-MARL is the fastest in inspecting the environment, therefore covering more informative cells. It is followed, in decreasing order, by GSA, MSA and MLP, which is reasonable since the three neural networks are in decreasing order of architecture complexity in terms of neural network

<sup>1</sup><https://github.com/EduardoSebastianRodriguez/phMARL>

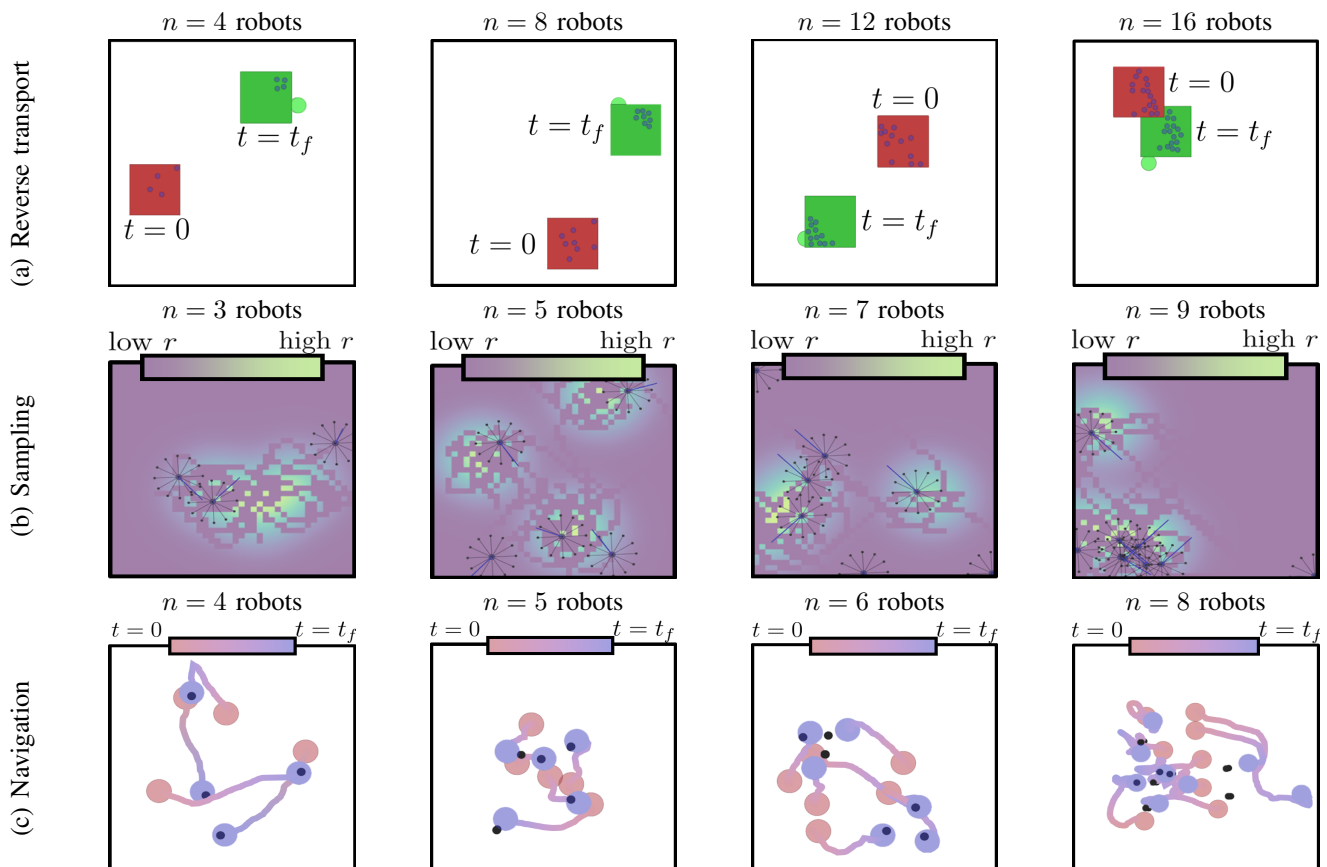


Fig. 5. Examples of multi-robot scenarios for different initial conditions and number of robots. It is interesting to see that some aspects of the environment do not scale with the team size, e.g., the size and weight of the box in the reverse transport scenario, the number of hot spots in the sampling scenario or the size of the arena in the navigation scenario.

TABLE I  
AVERAGED TRAINING CONVERGENCE CUMULATIVE REWARD FOR THE FOUR ABLATED METHODS. IN ALL THE CASES,  $n = 4$  ROBOTS ARE USED.

Method	Mean and std of $\bar{R}$ over 10 evaluation episodes		
	Reverse transport	Sampling	Navigation
pH-MARL	<b><math>213 \pm 21</math></b>	<b><math>161 \pm 41</math></b>	<b><math>-53 \pm 101</math></b>
MLP	$64 \pm 38$	$73 \pm 25$	$-280 \pm 98$
MSA	$57 \pm 43$	$82 \pm 32$	$-353 \pm 99$
GSA	$90 \pm 49$	$89 \pm 38$	$-204 \pm 87$

modules and input information. The navigation scenario is the simplest among the three. Nevertheless, pH-MARL is still the best because it better learns the collision avoidance constraint.

To assess the scalability of the different architectures, in Fig. 4 each trained neural network is evaluated with a different number of robots, showing the mean and standard deviation of  $\bar{R}$  over 10 episodes. The first conclusion is that pH-MARL and GSA scale well with the number of robots, achieving the same cumulative reward per robot for all team sizes. In contrast, MSA and MLP do not scale because their architectures considers directly the global observation and action vectors, so their modules are not ready to process an input vector of different dimension. On the other hand, pH-MARL achieves much better performance than the other networks in all the scenarios and team sizes, thus confirming the importance of using physics-informed priors to ease the learning. The single

exception is in the navigation example, where the performance deteriorates when the number of robots increases.

Fig. 5 provides some qualitative examples for the three scenarios and helps to understand some limitations of our approach. Beginning with the navigation scenario, we can see that the size of the arena does not scale with the number of robots, it is always  $2 \times 2\text{m}$ . Hence, taking into account that the robots have a radius of  $15\text{cm}$ , the space is very small to navigate towards the landmarks without colliding. According to the reward, the robots search for safe motions, so they prefer to avoid collisions rather than moving to their landmarks (Fig. 5, navigation with 8 robots). There are other features that do not scale in the reverse transport and sampling scenarios: size of the box, weight of the box, size of the arena and number of Gaussian modes. Nonetheless, pH-MARL is capable of generalizing, scaling and circumventing these issues and achieve the desired tasks. In the reverse transport scenario, even with 16 robots that are highly packed inside the box, the robots manage to push the box and avoid erratic movements caused by the low weight of the box. In the sampling scenario, robots learn to spread and coordinate to cover more cells when there are more robots. Interestingly, when there are a lot of robots ( $n = 9$ ), some robots move to the corners because they annoy the others by increasing the potential number of collisions.

Summing up, the combination of a port-Hamiltonian for-

mulation and self-attention mechanisms leads to superior performance and the desired scalability with the number of robots, learning control policies that are distributed by design and fully exploit the graph structure of the multi-robot system.

### B. Comparative results

We compare the performance of our proposed physics-informed multi-agent reinforcement learning approach with other state-of-the-art multi-agent reinforcement learning approaches. In particular, we compare with: Multi-Agent Deep Deterministic Policy Gradient (MADDPG) [57], Mean Field Actor Critic (MFAC) [59], Evolutionary Population Curriculum (EPC) [77] and Distributed multi-Agent Reinforcement Learning with One-hop Neighbors (DARL1N) [60]. The comparison results reported in this paper are extracted from [60].

We use the food collection, grassland and adversarial scenarios for the comparison. Following the same procedure in [60], for the scenarios with an adversarial team (grassland and adversarial), we first use MADDPG to learn the control policies of both teams. Then, the adversarial team control policy is frozen and the policy of the other team is learned using any of the aforementioned approaches.

Next, we assess the scalability of our proposed approach in this second series of scenarios. We train the other state-of-the-art approaches for each specific number of robots, ranging from 3 to 48 robots. In contrast, we train pH-MARL  $n = 4$  robots and evaluate the trained control policies with the other number of robots, without further training. Fig. 6 demonstrates that pH-MARL achieves better or similar results than the other approaches without further training the control policies. When the team size is close to the one used during training ( $n = 3, 6, 12$ ) pH-MARL surpasses the other methods in the three scenarios, proving the accuracy of combining a physics-informed description of the multi-robot team with self-attention mechanisms. When the team size is much greater than the one used during training (24, 48), pH-MARL outperforms (MADDPG, MFAC) or achieves similar results (EPC, DARL1N) as the state-of-the-art. Notably, pH-MARL outperforms all the state-of-the-art methods in the adversarial scenario even when  $n = 48$ , which is significant considering that they are all trained with  $n = 48$  robots except pH-MARL, which is trained with  $n = 4$  robots.

The reason why pH-MARL exhibits a slight drop in performance when  $n = 24, 48$  robots is the same discussed in the ablation experiments. There are some features of the scenarios, like the size of the arena, that do not scale with the number of robots. Robots are not trained to move in configurations that far from those experienced during training. How to design the control policy to be invariant to environmental changes is part of the future work. Qualitative examples can be found in the repository associated to the paper.

## VII. CONCLUSIONS

We proposed a novel reinforcement learning formulation where the single agent is the multi-robot graph. On the one hand, this allowed to explicitly consider the potential networked interactions among agents, going beyond the classical

assumptions of independent execution found in other multi-agent reinforcement learning approaches. On the other hand, this allowed to avoid non-stationarity issues found during training in other multi-robot learning setting. In particular, we designed a soft actor-critic algorithm to manage the networked and stochastic nature of distributed multi-robot policies, learning simultaneously the homogeneous distributed control policy for all the robots while respecting the policy  $k$ -hop factorization and the correlation among robots. Besides, the method exploits the collective knowledge of a centralized critic during training. To achieve the learning of scalable and distributed control policies by design, we proposed an interconnection and damping passivity-based control policy based on a port-Hamiltonian description of the multi-robot dynamics that preserves energy conservation laws and individual robot dynamics. To parameterized the controller, we proposed a set of self-attention-based neural networks that respects the desired distributed structure of the control policy and handles the time-varying available information at each robot.

We have conducted ablation studies and comparative simulations against other state-of-the-art multi-agent reinforcement learning approaches in six scenarios, covering a wide variety of cooperative and competitive behaviors such as collision avoidance, navigation, transport, evasion and monitoring. In all the cases, our proposed approach exhibits superior performance in terms of cumulative reward per robot and scalability. Our approach, without further training, scales and achieves the same performance of other methods that are trained, ad hoc, with a specific number of robots. Nevertheless, there is still room for improvement in terms of generalization with respect to environmental conditions such as stage size. These results lead to the following conclusion: the combination of physics-informed neural networks and reinforcement learning techniques is a promising research line to address multi-robot problems.

## APPENDIX A NETWORK PARAMETERS

The self-attention-based control policy in pH-MARL is parameterized as follows:

- $[\mathbf{R}\theta]_{ij}$ :  $W = 3$ ,  $h_w = [n_x, 16, 8]$ ,  $r_w = [8, 16, 8]$ ,  $d_w = [16, 8, 16]$ ; functions  $\beta = \text{sigmoid}$ ,  $\chi = \psi = \text{swish}$  [78].
- $[\mathbf{J}\theta]_{ij}$ :  $W = 3$ ,  $h_w = [n_x, 16, 8]$ ,  $r_w = [8, 16, 8]$ ,  $d_w = [16, 8, 16]$ ; functions  $\beta = \text{sigmoid}$ ,  $\chi = \psi = \text{swish}$  [78].
- $H_\theta^i$ :  $W = 3$  layers,  $h_w = [n_x, 16, 8]$ ,  $r_w = [16, 8, 8]$ ,  $d_w = [16, 8, 25]$ ; functions  $\beta = \text{sigmoid}$ ,  $\chi = \psi = \text{swish}$  [78].

For the variance network we use the same architecture of  $[\mathbf{R}\theta]_{ij}$  but with  $h_1 = n_x + n_u$  and  $d_W = 2$ . The other networks used in the ablation studies are as follows:

- MLP: the policy is a single multi-layer perceptron of size  $[n \times n_x, n \times n_u, n \times n_u]$  with swish hidden activation function and linear output. For the variance network we use the same architecture but with size  $[n(n_x + n_u), n \times n_u, n \times n_u]$ .
- MSA: the policy is a single multi-layer perceptron of size  $[n \times n_x, n \times n_x]$  with linear output followed by a self-attention layer where query, key and values are directly

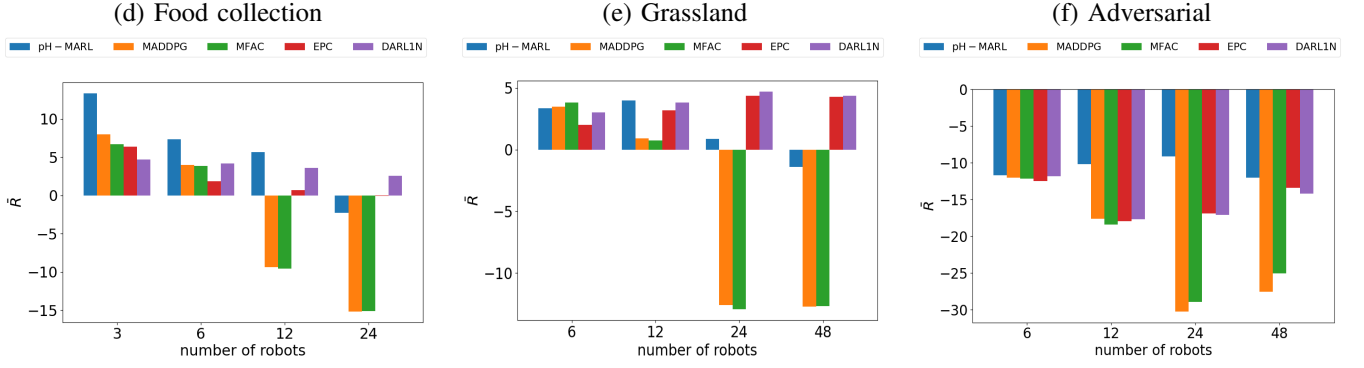


Fig. 6. Comparison of our proposed physics-informed multi-agent reinforcement learning approach with other state-of-the-art approaches. pH-MARL is only trained with  $n = 4$  robots and deployed with different team sizes, while the state-of-the-art control policies are trained for each specific number of robots.

the feature vector from the multi-layer perceptron, and an additional multi-layer perceptron of size  $[n \times n_x, n \times n_u]$  with linear output. For the variance network we use the same architecture but with size  $[n(n_x + n_u), n \times n_u]$  for the first multi-layer perceptron.

- GSA: the policy is the same one used to predict  $[\mathbf{R}_\theta]_{i,j}$  but with  $d_W = 2$ . For the variance network we use the same architecture but  $h_1 = n_x + n_u$ .

The  $Q_{\Pi_\theta}(s_t, \mathbf{a}_t)$  function is always parameterized as a multi-layer perceptron with layers of size  $[n(n_x + n_u), 2n(n_x + n_u), n(n_x + n_u), (n_x + n_u), 1]$  with swish [78] activation functions except the last layer, that is linear.

The food collection, grassland, and adversarial scenarios use a neural network to pre-process the observation vector to move from a time-varying observation size to a fixed state size compatible with the control policies. To do so, the state is a concatenation of the position (2-dimensional vector), velocity (2-dimensional vector), aliveness (boolean quantity), closest goal relative distance (2-dimensional vector) and a 2-dimensional feature vector provided by a neural network. The neural network is composed by a multi-layer perceptron with no hidden layers of size  $[n_x - 2, 2]$  and swish activation function, a self-attention layer of size  $h_w = r_w = d_w = 2$ , and another multi-layer perceptron with no hidden layers of size  $[2, 2]$  and linear output.

## APPENDIX B

### SOFT ACTOR-CRITIC HYPERPARAMETERS

The following table details the parameterization of the soft actor-critic algorithm for the different scenarios.

TABLE II: Soft actor-critic hyperparameters.

Parameter	Scenario	Value
optimizer	all	Adam [79]
$r_{comm}$	reverse transport, navigation	0.45m
	sampling	0.75m
	food collection, grassland, adversarial	0.15m

Continued on next page

TABLE II: Soft actor-critic hyperparameters. (Continued)

$n$ training	reverse transport, sampling, navigation	4
	food collection, grassland, adversarial	8
# parallel environments	all	96
shared $r$	all	True
maximum steps per episode	reverse transport, navigation, food collection, grassland, adversarial	400
	sampling	1000
replay buffer size	all	$2 \times 10^6$
initial random steps	all	$10^3$
$\gamma$	all	0.99
$\alpha_0$	all	5
$\alpha_{min}$	all	0.1
$\alpha_{max}$	all	10
$\rho$	all	0.005
learning rate $\alpha$	all	$10^{-5}$
learning rate	all	$10^{-4}$
batch size	all	1024
# training steps	navigation, reverse transport, sampling, food collection, grassland	$2 \times 10^6$
	adversarial	$6 \times 10^5$
clip gradients	all	False
reward scaling	all	False
$\sigma_{min}$	all	$e^{-5}$
$\sigma_{max}$	all	$e^2$

Continued on next page

TABLE II: Soft actor-critic hyperparameters. (Continued)

landmark mass	sampling, navigation, food collection, grassland, adversarial	default
	reverse transport	1
evaluation interval	all	$10^4$
# evaluation episodes per interval	all	10

## REFERENCES

- [1] N. Atanasov, J. Le Ny, K. Daniilidis, and G. J. Pappas, “Decentralized active information acquisition: Theory and application to multi-robot SLAM,” in *IEEE International Conference on Robotics and Automation*, 2015, pp. 4775–4782.
- [2] Y. Tian, Y. Chang, F. H. Arias, C. Nieto-Granda, J. P. How, and L. Carlone, “Kimera-multi: Robust, distributed, dense metric-semantic SLAM for multi-robot systems,” *IEEE Transactions on Robotics*, 2022.
- [3] X. Kan, T. C. Thayer, S. Carpin, and K. Karydis, “Task planning on stochastic aisle graphs for precision agriculture,” *IEEE Robotics and Automation Letters*, vol. 6, no. 2, pp. 3287–3294, 2021.
- [4] A. Pierson and M. Schwager, “Bio-inspired non-cooperative multi-robot herding,” in *IEEE International Conference on Robotics and Automation*, 2015, pp. 1843–1849.
- [5] E. Sebastián and E. Montijano, “Multi-robot implicit control of herds,” in *IEEE International Conference on Robotics and Automation*, 2021, pp. 1601–1607.
- [6] E. Sebastián, E. Montijano, and C. Sagüés, “Adaptive multirobot implicit control of heterogeneous herds,” *IEEE Transactions on Robotics*, 2022.
- [7] L. Heintzman, A. Hashimoto, N. Abaid, and R. K. Williams, “Anticipatory planning and dynamic lost person models for human-robot search and rescue,” in *IEEE International Conference on Robotics and Automation*, 2021, pp. 8252–8258.
- [8] M. J. Mataric, “Reinforcement learning in the multi-robot domain,” *Autonomous Robots*, vol. 1, no. 4, pp. 73–83, 1997.
- [9] L. Matignon, G. J. Laurent, and N. Le Fort-Piat, “Hysteretic q-learning: an algorithm for decentralized reinforcement learning in cooperative multi-agent teams,” in *IEEE/RSJ International Conference on Intelligent Robots and Systems*, 2007, pp. 64–69.
- [10] L. Matignon, L. Jeanpierre, and A.-I. Mouaddib, “Coordinated multi-robot exploration under communication constraints using decentralized markov decision processes,” in *Proceedings of the AAAI Conference on Artificial Intelligence*, vol. 26, no. 1, 2012, pp. 2017–2023.
- [11] S. Munikoti, D. Agarwal, L. Das, M. Halappanavar, and B. Natarajan, “Challenges and opportunities in deep reinforcement learning with graph neural networks: A comprehensive review of algorithms and applications,” *IEEE Transactions on Neural Networks and Learning Systems*, 2023.
- [12] Á. Serra-Gómez, H. Zhu, B. Brito, W. Böhmer, and J. Alonso-Mora, “Learning scalable and efficient communication policies for multi-robot collision avoidance,” *Autonomous Robots*, pp. 1–23, 2023.
- [13] Y. L. Lo, C. S. de Witt, S. Sokota, J. N. Foerster, and S. Whiteson, “Cheap talk discovery and utilization in multi-agent reinforcement learning,” in *The Eleventh International Conference on Learning Representations*, 2023.
- [14] G. Qu, A. Wierman, and N. Li, “Scalable reinforcement learning for multiagent networked systems,” *Operations Research*, vol. 70, no. 6, pp. 3601–3628, 2022.
- [15] T. Beckers, T. Z. Jiahao, and G. J. Pappas, “Learning switching port-hamiltonian systems with uncertainty quantification,” *arXiv preprint arXiv:2305.09689*, 2023.
- [16] C. Neary and U. Topcu, “Compositional learning of dynamical system models using port-hamiltonian neural networks,” in *Learning for Dynamics and Control Conference*. PMLR, 2023, pp. 679–691.
- [17] E. Sebastián, N. Duong, N. Atanasov, E. Montijano, and C. Sagüés, “LEMURS: Learning Distributed Multi-Robot Interactions,” in *IEEE International Conference on Robotics and Automation*, 2023, pp. 7713–7719.
- [18] T. X. Nghiem, J. Drgoňa, C. Jones, Z. Nagy, R. Schwan, B. Dey, A. Chakrabarty, S. Di Cairano, J. A. Paulson, A. Carron, *et al.*, “Physics-informed machine learning for modeling and control of dynamical systems,” *arXiv preprint arXiv:2306.13867*, 2023.
- [19] S. Sanyal and K. Roy, “Ramp-net: A robust adaptive mpc for quadrotors via physics-informed neural network,” in *IEEE International Conference on Robotics and Automation*, 2023, pp. 1019–1025.
- [20] C. Rodwell and P. Tallapragada, “Physics-informed reinforcement learning for motion control of a fish-like swimming robot,” *Scientific Reports*, vol. 13, no. 1, p. 10754, 2023.
- [21] S. Cuomo, V. S. Di Cola, F. Giampaolo, G. Rozza, M. Raissi, and F. Piccialli, “Scientific machine learning through physics-informed neural networks: Where we are and what’s next,” *Journal of Scientific Computing*, vol. 92, no. 3, p. 88, 2022.
- [22] Y. Xu, S. Koltz, J. Boakye, P. Gardoni, and P. Wang, “Physics-informed machine learning for reliability and systems safety applications: State of the art and challenges,” *Reliability Engineering & System Safety*, p. 108900, 2022.
- [23] D. Bloembergen, K. Tuyls, D. Hennes, and M. Kaisers, “Evolutionary dynamics of multi-agent learning: A survey,” *Journal of Artificial Intelligence Research*, vol. 53, pp. 659–697, 2015.
- [24] P. Long, T. Fan, X. Liao, W. Liu, H. Zhang, and J. Pan, “Towards optimally decentralized multi-robot collision avoidance via deep reinforcement learning,” in *IEEE International Conference on Robotics and Automation*, 2018, pp. 6252–6259.
- [25] S. H. Semnani, H. Liu, M. Everett, A. De Ruiter, and J. P. How, “Multi-agent motion planning for dense and dynamic environments via deep reinforcement learning,” *IEEE Robotics and Automation Letters*, vol. 5, no. 2, pp. 3221–3226, 2020.
- [26] A. Y. Ng, S. Russell, *et al.*, “Algorithms for inverse reinforcement learning,” in *International Conference on Machine Learning*, vol. 1, 2000, p. 2.
- [27] S. Dasari, F. Ebert, S. Tian, S. Nair, B. Bucher, K. Schmeckpeper, S. Singh, S. Levine, and C. Finn, “Robonet: Large-scale multi-robot learning,” in *Conference on Robot Learning*, 2020, pp. 885–897.
- [28] K. Bogert and P. Doshi, “Multi-robot inverse reinforcement learning under occlusion with estimation of state transitions,” *Artificial Intelligence*, vol. 263, pp. 46–73, 2018.
- [29] R. Han, S. Chen, and Q. Hao, “Cooperative multi-robot navigation in dynamic environment with deep reinforcement learning,” in *IEEE International Conference on Robotics and Automation*, 2020, pp. 448–454.
- [30] I. Gharbi, J. Kuckling, D. G. Ramos, and M. Birattari, “Show me what you want: Inverse reinforcement learning to automatically design robot swarms by demonstration,” *arXiv preprint arXiv:2301.06864*, 2023.
- [31] H. Zhu, F. M. Claramunt, B. Brito, and J. Alonso-Mora, “Learning interaction-aware trajectory predictions for decentralized multi-robot motion planning in dynamic environments,” *IEEE Robotics and Automation Letters*, vol. 6, no. 2, pp. 2256–2263, 2021.
- [32] S. Zhou, M. J. Phielipp, J. A. Sefair, S. I. Walker, and H. B. Amor, “Clone swarms: Learning to predict and control multi-robot systems by imitation,” in *IEEE/RSJ International Conference on Intelligent Robots and Systems*, 2019, pp. 4092–4099.
- [33] G. Qu, A. Wierman, and N. Li, “Scalable reinforcement learning of localized policies for multi-agent networked systems,” in *Learning for Dynamics and Control*. PMLR, 2020, pp. 256–266.
- [34] V. Zambaldi, D. Raposo, A. Santoro, V. Bapst, Y. Li, I. Babuschkin, K. Tuyls, D. Reichert, T. Lillicrap, E. Lockhart, *et al.*, “Deep reinforcement learning with relational inductive biases,” in *International conference on learning representations*, 2018.
- [35] S. Iqbal and F. Sha, “Actor-attention-critic for multi-agent reinforcement learning,” in *International conference on machine learning*. PMLR, 2019, pp. 2961–2970.
- [36] G. Li, B. Jiang, H. Zhu, Z. Che, and Y. Liu, “Generative attention networks for multi-agent behavioral modeling,” in *Proceedings of the AAAI Conference on Artificial Intelligence*, vol. 34, no. 05, 2020, pp. 7195–7202.
- [37] P. Parnika, R. B. Diddigi, S. K. R. Danda, and S. Bhatnagar, “Attention actor-critic algorithm for multi-agent constrained co-operative reinforcement learning,” in *International Conference on Autonomous Agents and Multiagent Systems*, 2021.
- [38] A. Marino, C. Pacchierotti, and P. R. Giordano, “On the stability of gated graph neural networks,” *arXiv preprint arXiv:2305.19235*, 2023.
- [39] Q. Li, W. Lin, Z. Liu, and A. Prorok, “Message-aware graph attention networks for large-scale multi-robot path planning,” *IEEE Robotics and Automation Letters*, vol. 6, no. 3, pp. 5533–5540, 2021.

- [40] A. Khan, E. Tolstaya, A. Ribeiro, and V. Kumar, "Graph policy gradients for large scale robot control," in *Conference on Robot Learning*, 2020, pp. 823–834.
- [41] E. Tolstaya, F. Gama, J. Paulos, G. Pappas, V. Kumar, and A. Ribeiro, "Learning decentralized controllers for robot swarms with graph neural networks," in *Conference on Robot Learning*, 2020, pp. 671–682.
- [42] E. Tolstaya, J. Paulos, V. Kumar, and A. Ribeiro, "Multi-robot coverage and exploration using spatial graph neural networks," in *IEEE/RSJ International Conference on Intelligent Robots and Systems*, 2021, pp. 8944–8950.
- [43] F. Yang and N. Matni, "Communication topology co-design in graph recurrent neural network based distributed control," in *IEEE Conference on Decision and Control*, 2021, pp. 3619–3626.
- [44] F. Gama, Q. Li, E. Tolstaya, A. Prorok, and A. Ribeiro, "Synthesizing decentralized controllers with graph neural networks and imitation learning," *IEEE Transactions on Signal Processing*, vol. 70, pp. 1932–1946, 2022.
- [45] L. Kuyer, S. Whiteson, B. Bakker, and N. Vlassis, "Multiagent reinforcement learning for urban traffic control using coordination graphs," in *Machine Learning and Knowledge Discovery in Databases: European Conference*. Springer, 2008, pp. 656–671.
- [46] L. Buşoniu, R. Babuška, and B. De Schutter, "Multi-agent reinforcement learning: An overview," *Innovations in multi-agent systems and applications-1*, pp. 183–221, 2010.
- [47] O. Vinyals, T. Ewalds, S. Bartunov, P. Georgiev, A. S. Vezhnevets, M. Yeo, A. Makhzani, H. Küttler, J. Agapiou, J. Schrittwieser, et al., "Starcraft ii: A new challenge for reinforcement learning," *arXiv preprint arXiv:1708.04782*, 2017.
- [48] B. Ellis, S. Moalla, M. Samvelyan, M. Sun, A. Mahajan, J. N. Foerster, and S. Whiteson, "SMACv2: An improved benchmark for cooperative multi-agent reinforcement learning," *arXiv preprint arXiv:2212.07489*, 2022.
- [49] S. Gronauer and K. Diepold, "Multi-agent deep reinforcement learning: a survey," *Artificial Intelligence Review*, pp. 1–49, 2022.
- [50] A. Oroojlooy and D. Hajinezhad, "A review of cooperative multi-agent deep reinforcement learning," *Applied Intelligence*, vol. 53, no. 11, pp. 13 677–13 722, 2023.
- [51] L. Matignon, G. J. Laurent, and N. Le Fort-Piat, "Independent reinforcement learners in cooperative markov games: a survey regarding coordination problems," *The Knowledge Engineering Review*, vol. 27, no. 1, pp. 1–31, 2012.
- [52] G. Papoudakis, F. Christianos, A. Rahman, and S. V. Albrecht, "Dealing with non-stationarity in multi-agent deep reinforcement learning," *arXiv preprint arXiv:1906.04737*, 2019.
- [53] W. Böhmer, V. Kurin, and S. Whiteson, "Deep coordination graphs," in *International Conference on Machine Learning*. PMLR, 2020, pp. 980–991.
- [54] T. Haarnoja, A. Zhou, K. Hartikainen, G. Tucker, S. Ha, J. Tan, V. Kumar, H. Zhu, A. Gupta, P. Abbeel, et al., "Soft actor-critic algorithms and applications," *arXiv preprint arXiv:1812.05905*, 2018.
- [55] T. P. Lillicrap, J. J. Hunt, A. Pritzel, N. Heess, T. Erez, Y. Tassa, D. Silver, and D. Wierstra, "Continuous control with deep reinforcement learning," *arXiv preprint arXiv:1509.02971*, 2015.
- [56] J. Schulman, F. Wolski, P. Dhariwal, A. Radford, and O. Klimov, "Proximal policy optimization algorithms," *arXiv preprint arXiv:1707.06347*, 2017.
- [57] R. Lowe, Y. I. Wu, A. Tamar, J. Harb, P. Abbeel, and I. Mordatch, "Multi-agent actor-critic for mixed cooperative-competitive environments," *Advances in neural information processing systems*, vol. 30, 2017.
- [58] J. Bloom, P. Paliwal, A. Mukherjee, and C. Pinciroli, "Decentralized multi-agent reinforcement learning with global state prediction," *arXiv preprint arXiv:2306.12926*, 2023.
- [59] Y. Yang, R. Luo, M. Li, M. Zhou, W. Zhang, and J. Wang, "Mean field multi-agent reinforcement learning," in *International Conference on Machine Learning*. PMLR, 2018, pp. 5571–5580.
- [60] B. Wang, J. Xie, and N. Atanasov, "DARLIN: Distributed multi-agent reinforcement learning with one-hop neighbors," in *IEEE/RSJ International Conference on Intelligent Robots and Systems*, 2022.
- [61] Y. Motokawa and T. Sugawara, "Interpretability for conditional coordinated behavior in multi-agent reinforcement learning," *arXiv preprint arXiv:2304.10375*, 2023.
- [62] R. Kortvelesy and A. Prorok, "QGNN: Value Function Factorisation with Graph Neural Networks," *arXiv preprint arXiv:2205.13005*, 2022.
- [63] Y. Hu, J. Fu, and G. Wen, "Graph soft actor-critic reinforcement learning for large-scale distributed multirobot coordination," *IEEE transactions on neural networks and learning systems*, 2023.
- [64] P. Zhao and Y. Liu, "Physics informed deep reinforcement learning for aircraft conflict resolution," *IEEE Transactions on Intelligent Transportation Systems*, vol. 23, no. 7, pp. 8288–8301, 2021.
- [65] G. Sartoretti, Y. Wu, W. Paivine, T. S. Kumar, S. Koenig, and H. Choset, "Distributed reinforcement learning for multi-robot decentralized collective construction," in *Distributed Autonomous Robotic Systems: The 14th International Symposium*. Springer, 2019, pp. 35–49.
- [66] A. Van Der Schaft and D. Jeltsema, "Port-Hamiltonian systems theory: An introductory overview," *Foundations and Trends in Systems and Control*, vol. 1, no. 2-3, pp. 173–378, 2014.
- [67] L. Furieri, C. L. Galimberti, M. Zakwan, and G. Ferrari-Trecate, "Distributed neural network control with dependability guarantees: a compositional port-hamiltonian approach," in *Learning for Dynamics and Control Conference*, 2022, pp. 571–583.
- [68] C. L. Galimberti, L. Furieri, L. Xu, and G. Ferrari-Trecate, "Hamiltonian deep neural networks guaranteeing nonvanishing gradients by design," *IEEE Transactions on Automatic Control*, vol. 68, no. 5, pp. 3155–3162, 2023.
- [69] G. Shi, W. Hönig, Y. Yue, and S.-J. Chung, "Neural-swarm: Decentralized close-proximity multirotor control using learned interactions," in *IEEE International Conference on Robotics and Automation*, 2020, pp. 3241–3247.
- [70] A. Vaswani, N. Shazeer, N. Parmar, J. Uszkoreit, L. Jones, A. N. Gomez, E. Kaiser, and I. Polosukhin, "Attention is all you need," *Advances in Neural Information Processing Systems*, vol. 30, 2017.
- [71] A. J. van der Schaft, "Port-Hamiltonian systems: network modeling and control of nonlinear physical systems," in *Advanced dynamics and control of structures and machines*. Springer, 2004, pp. 127–167.
- [72] G. Blankenstein, R. Ortega, and A. J. Van Der Schaft, "The matching conditions of controlled lagrangians and ida-passivity based control," *International Journal of Control*, vol. 75, no. 9, pp. 645–665, 2002.
- [73] T. Haarnoja, A. Zhou, P. Abbeel, and S. Levine, "Soft actor-critic: Off-policy maximum entropy deep reinforcement learning with a stochastic actor," in *International conference on machine learning*. PMLR, 2018, pp. 1861–1870.
- [74] M. Bettini, R. Kortvelesy, J. Blumenkamp, and A. Prorok, "VMAS: a vectorized multi-agent simulator for collective robot learning," *arXiv preprint arXiv:2207.03530*, 2022.
- [75] T. Haarnoja, S. Ha, A. Zhou, J. Tan, G. Tucker, and S. Levine, "Learning to walk via deep reinforcement learning," *arXiv preprint arXiv:1812.11103*, 2018.
- [76] I. Mordatch and P. Abbeel, "Emergence of grounded compositional language in multi-agent populations," in *Proceedings of the AAAI conference on artificial intelligence*, vol. 32, no. 1, 2018.
- [77] Q. Long, Z. Zhou, A. Gupta, F. Fang, Y. Wu, and X. Wang, "Evolutionary population curriculum for scaling multi-agent reinforcement learning," in *International Conference on Learning Representations*, 2019.
- [78] P. Ramachandran, B. Zoph, and Q. V. Le, "Searching for activation functions," *arXiv preprint arXiv:1710.05941*, 2017.
- [79] D. P. Kingma and J. Ba, "Adam: A method for stochastic optimization," in *International Conference for Learning Presentations*, 2015.